PROCEEDINGS OF SPIE

SPIEDigitalLibrary.org/conference-proceedings-of-spie

# Photoacoustic molecular imaging of angiogenesis using theranostic αvβ3-targeted copper nanoparticles incorporating a sn-2 lipase-labile fumagillin prodrug

Ruiying Zhang, Xin Cai, Xiaoxia Yang, Angana Senpan, John S. Allen, et al.

Ruiying Zhang, Xin Cai, Xiaoxia Yang, Angana Senpan, John S. Allen, Dipanjan Pan, Gregory M. Lanza, Lihong V. Wang, "Photoacoustic molecular imaging of angiogenesis using theranostic αvβ3-targeted copper nanoparticles incorporating a sn-2 lipase-labile fumagillin prodrug," Proc. SPIE 8943, Photons Plus Ultrasound: Imaging and Sensing 2014, 89435I (3 March 2014); doi: 10.1117/12.2041120

SPIE.

Event: SPIE BiOS, 2014, San Francisco, California, United States

# Photoacoustic molecular imaging of angiogenesis using theranostic $\alpha_v\beta_3$-targeted copper nanoparticles incorporating a sn-2 lipase-labile fumagillin prodrug

Ruiying Zhang[a] , Xin Cai[a], Xiaoxia Yang[b], Angana Senpan[b], John S. Allen[b], Dipanjan Pan[c] ,Gregory M. Lanza[b] and Lihong V. Wang[a*]

[a]Optical Imaging Laboratory, Department of Biomedical Engineering, Washington University in St. Louis, St. Louis, MO USA 63130;

[b]Department of Medicine, Washington University School of Medicine in St. Louis, St. Louis, MO USA 63108;

[c]Department of Bioengineering, University of Illinois at Urbana-Champaign, Champaign, IL USA, 61801

## ABSTRACT

Photoacoustic (PA) tomography imaging is an emerging, versatile, and noninvasive imaging modality, which combines the advantages of both optical imaging and ultrasound imaging. It opens up opportunities for noninvasive imaging of angiogenesis, a feature of skin pathologies including cancers and psoriasis. In this study, high-density copper oleate encapsulated within a phospholipid surfactant (CuNPs) generated a soft nanoparticle with PA contrast comparable to gold. Within the near-infrared window, the copper nanoparticles can provide a signal more than 7 times higher that of blood. $\alpha_v\beta_3$-integrin targeting of CuNPs in a Matrigel mouse model demonstrated prominent PA contrast enhancement of the neovasculature compared to mice given nontargeted or competitively inhibited CuNPs. Incorporation of a sn-2 lipase-labile fumagillin prodrug into the CuNPs produced marked antiangiogenesis in the same model, demonstrating the theranostic potential of a PA agent for the first time in vivo. With a PA signal comparable to gold-based nanoparticles yet a lower cost and demonstrated drug delivery potential, $\alpha_v\beta_3$-targeted CuNPs hold great promise for the management of skin pathologies with neovascular features.

**Keywords:** Copper nanoparticles, $\alpha_v\beta_3$-targeted, photoacoustic molecular imaging, angiogenesis, antiangiogenic therapy, fumagillin prodrug

## 1. INTRODUCTION

Photoacoustic (PA) imaging, combining the advantage of ultrasound imaging and optical imaging, has attracted much attention. Based on the detection of optical absorbers such as hemoglobin, it offers high depth-to-resolution with different scales, ranging from organelles to organs. Previous studies have confirmed the potential of PA imaging with exogenous contrast agents to quantify vascularization, oxygen saturation and angiogenesis. [1-6] For example, gold nanoparticles, with their large absorption cross section, can be tuned to the optical window, which minimizes endogenous absorption and maximizes imaging depth. The conjugation capability of nanoparticles enables biomarker targeting for molecular imaging and drug delivery. [7]

However, because of the high cost of gold nanoparticles, their clinical use is discouraged. Furthermore, manufacturing them requires complicated morphology and expensive chemistries. An alternative low-cost contrast agent is desirable, but has not been reported yet. In this paper, we hypothesize a new kind of vascular-constrained, $\alpha_v\beta_3$-targeted copper nanoparticles (CuNPs) for the discrimination of neovasculature. As copper is cheaper than gold, these nanoparticles are expected to provide an inexpensive and effective alternative optical contrast agent for PA imaging. In this work, the PA imaging was performed with our home-made PA deep imaging system. The data and images from different groups of mice after the injection of copper nanoparticles were compared and analyzed.

*lhwang@biomed.wustl.edu

Photons Plus Ultrasound: Imaging and Sensing 2014, edited by Alexander A. Oraevsky, Lihong V. Wang,
Proc. of SPIE Vol. 8943, 89435I · © 2014 SPIE · CCC code: 1605-7422/14/$18 · doi: 10.1117/12.2041120

## 2. METHODS

### 2.1 Synthesis of nanoparticles

The synthesis of copper nanoparticles was performed similarly to the synthesis of gold nanoparticles reported [8], except that the Cu-oleate was immersed in almond oil instead of octanethiol-coated gold nanoparticles. Fumagilin (1 mol %) was incorporated into the lipid layer of the CuNPs as shown in Fig. 1.

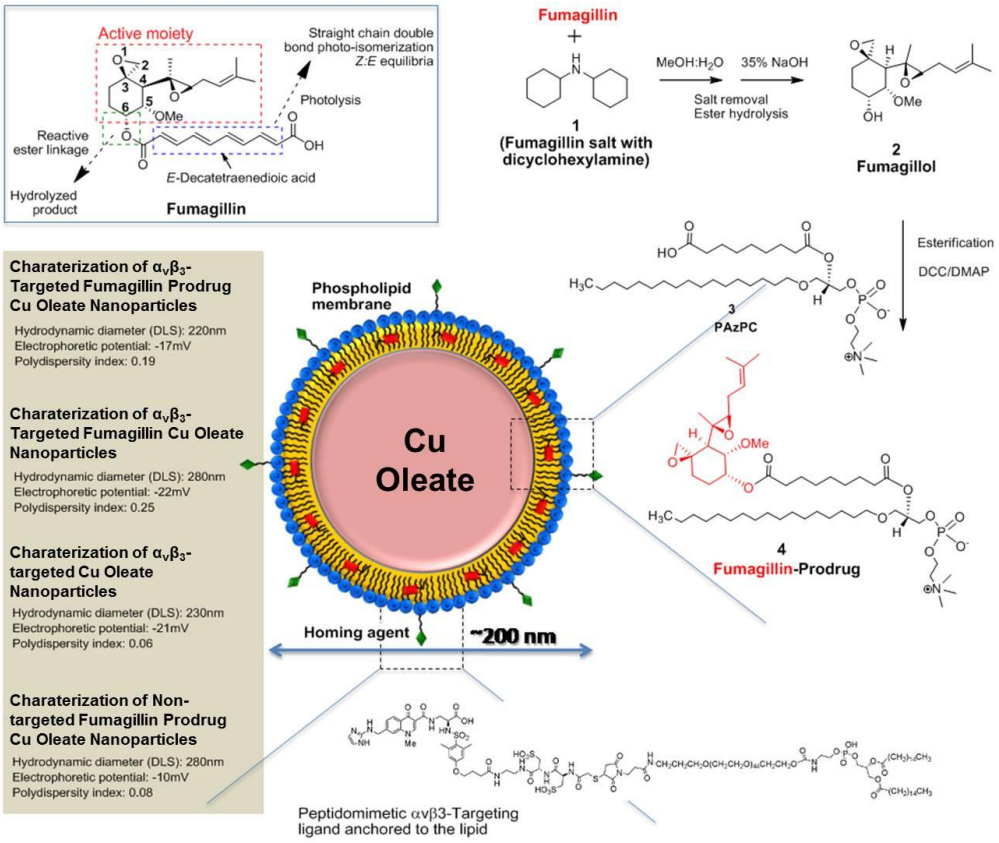


Fig. 1 Schematic of the copper nanoparticles incorporating fumagillin

### 2.2 Matrigel model of angiogenesis

Athymic nude-mice with body weights ranging from 23 to 27 g were used. The anesthesia induction utilized ketamine (100 mg/ml) and xylazine (20 mg/ml) that was maintained with 0.5% -1% isoflurane in oxygen on a ventilator. Matrigel (0.5 ml, BI; Biosciences, San Jose, CA, USA) enriched with fibroblast growth factor -2 (500 nm/ml; Sigma-Aldrich, St. Louis, MO, USA) and heparin was implanted subcutaneously along the flank. The nude mice (N = 15) were randomly distributed into four groups and injected with: 1) $\alpha_v\beta_3$ CuNPs w/o fumagilin (N = 3) right before PA imaging; 2) $\alpha_v\beta_3$/fumagilin CuNPs (N = 3) on day 11 and day 15 as antiangiogenesis therapy, and $\alpha_v\beta_3$ CuNPs w/o fumagilin (N = 3) right before PA imaging; 3) $\alpha_v\beta_3$ blank particles and 10 mins later, treated with $\alpha_v\beta_3$ CuNPs w/o fumagilin (N = 3) right before PA imaging; 4) non-targeted CuNPs right before PA imaging. PA imaging was performed before the injection, and serially over 3~5 h post-injection on day 17-19. Animal studies were performed under a protocol approved by Washington University Medical School Animal Studies Committee.

### 2.3 PA imaging system

Using dark-field ring-shaped illumination, a reflection-mode PA imaging system[9] was pumped by a Q- switched Nd:YAG (LS-2137; Lotis TII) laser with <15-ns pulse duration and a 10-Hz pulse repetition rate. The light energy on the sample surface was controlled to conform to the American National Standards Institute standard for maximum

permissible exposure. A 10 MHz central frequency, spherically focused (2.54-cm focus length, 1.91-cm diameter active area element, and 72% bandwidth) ultrasonic transducer (V308; Panametrics-NDT, Waltham, MA, USA) was used to acquire the generated PA signals. The signal was amplified by a low-noise amplifier (5072PR; Panametrics-NDT), and recorded using a digital oscilloscope (TDS 5054; Tektronix, Beaverton, OR, USA) with 50-MHz sampling. PA signal fluctuations due to pulse-to-pulse energy variation were compensated for by signals from a photodiode (DET110; Thorlabs, Newton, NJ, USA), which sampled the energy of each laser pulse. A linear translation stage (XY-6060; Danaher Motion, Rad- ford, VA, USA) was used for raster scanning to obtain 3-D PA data. A computer controlled the stage and synchronized it with the data acquisition. To shorten the data acquisition time, a continuous scan was used without signal averaging. Typical scanning values are as follows: voxel dimension, 0.1 × 0.2 mm; laser pulse repetition rate, 10 Hz; acquisition time, ~20 min. *In vivo* imaging was performed using ventilated anesthetized mice with shaved flanks, constantly warmed to 37 ℃ by a heating block and positioned immediately beneath the transparent clear membrane. The resolution of the system using a 10 MHz transducer was tested prior to imaging. It was shown that at the focus, the resolution was around 137 μm.

An angiogenesis index, defined as the cross-product of blood vessel pixel number and the total PA signal from those pixels, was used to quantify the visualization of angiogenesis. The angiogenesis index was normalized to that of the pretreatment during the analysis.

## 3. RESULTS

The efficacy of CuNPs was compared with blood in the near-infrared (NIR) window. The PA signal was obtained from fresh bovine blood (Quad Five, Cat. #905, Hct., 30%~ 50%) and CuNPs (2 wt/vol%) filled in a tygon tube (i.d. = 510μm) at laser wavelength from 725 nm to 830 nm. Fig. 2(a) and (b) show that the PA signal from CuNPs was clearly much stronger than that from blood over the entire spectrum. Also, when the laser is tuned to 770 nm, the PA signal of the CuNPs reaches its peak. Considering the ratio of PA signal and laser energy at different wavelengths, 770 nm was chosen. Shown in Fig. 2(c), at 770 nm, the peak-to-peak PA signal amplitude obtained from CuNPs was ~2.5 V, compared to ~0.32 V peak-to-peak PA signal from blood alone, which is about 7 times stronger than that from blood at 770 nm wavelength. The typical preparation of CuNPs (2 wt/vol%) provided an SNR of 36 dB at 770 nm in vitro. The high ratio of PA signal amplitude derived from CuNPs over blood suggests potential clinical use for intravascular and extravascular applications within the NIR window.

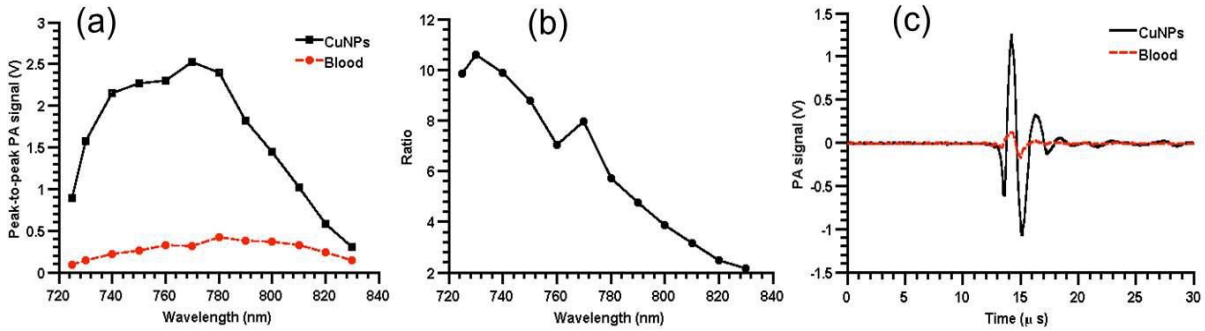


Fig.2 (a) Comparative PA spectra of CuNPs and blood over 730-830 nm NIR wavelength range. (b) Ratio of the peak-to-peak PA signal amplitudes generated from CuNPs to those of blood over 730-830 nm. (c)PA spectroscopy signals generated from a tygon tube (i.d. = 510 μm) filled with CuNPs. The laser was tuned to 770 nm wavelength The results were obtained using deep PA system without calibration of laser energy under different wavelength.

A time course study revealed gradual signal enhancement with $\alpha_v\beta_3$-targeted CuNPs post-treatment in a mouse Matrigel-plug model, at every 0.5 h interval up to 3.5 h. A nude mouse bearing 17-d implant was treated intravenously with $\alpha_v\beta_3$-targeted CuNPs. The PA signal changes in the Matrigel plug area after the injection of $\alpha_v\beta_3$-targeted CuNPs were monitored serially over 3.5 h. (Fig. 3). Signals from individual vessels were enhanced with time. Neovessels and angiogenic sprouts, which cannot be visualized with hemoglobin alone, were observed. It can be concluded that as time increases, $\alpha_v\beta_3$-targeted CuNPs penetrate into the Matrigel plug and target angiogenic vessels. Some angiogenic vessels seen in the Matrigel plug were still under development, which would make them below the resolution of PA. Fig.3 (e)

illustrates an overall signal enhancement of all the vessels in the Matrigel plug area, suggesting all the vessels in the image may be angiogenic vessels.

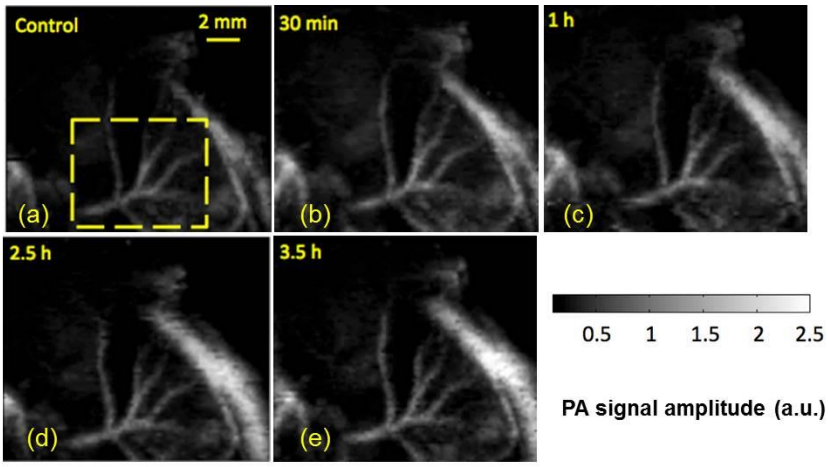


Fig.3 After 17d bearing Matrigel plug (0.5 ml), a nude mouse was imaged by PA. (a) PA maximum amplitude projection (MAP) image of the area with Matrigel plug. This is a control image. (b) - (e) A time course study was conducted after the injection of targeted CuNPs. PA images were taken every 0.5 h up to 3.5 h. For all PA images, PA wavelength = 770 nm and scale bar = 2 mm, field of view, 14 ×17 mm.

The effectiveness of fumagillin therapy was proved by a time course study with PA, shown in Fig. 4. Signals from the Matrigel plug area after the fumagillin therapy were monitored over 4 h. Fewer vessels can be visualized both before and after the injection of $\alpha_v\beta_3$-targeted CuNPs compared with those in Fig. 3. Also, both the number and the signal amplitude of vessels in the PA image stayed the same after the injection. These results suggest that the fumagillin therapy with $\alpha_v\beta_3$-targeted CuNPs successfully suppressed the level of neovasculature.

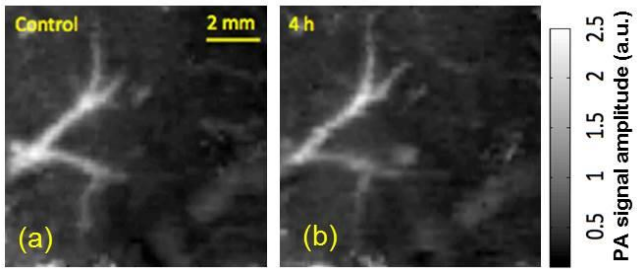


Fig. 4. After 17 d bearing Matrigel plug and undergoing fumagillin therapy, the nude mouse was imaged by PA. (a) PA maximum amplitude projection (MAP) image of the area of Matrigel plug. This is a control image. (b) PA MAP image taken at 4 h after the injection of CuNPs. For all PA images, PA wavelength = 770 nm and scale bar = 2 mm, field of view, 10 ×10 mm

The aniogenesis index was calculated to quantify the PA image change between different groups. Fig. 5 shows the angiogenesis curve versus time: angiogenesis index increased with time for $\alpha_v\beta_3$-targted CuNPs group but almost remains unchanged or changed little for the other three groups.

## 4. DISCUSSIONS

As an essential biomarker of tumors and progression of cardiovascular disease, angiogenesis provides us with information about disease progression and intensity[10]. Photoacoustic (PA) imaging, which closes the resolution limit of in vitro microscopic methods and existing clinical methods, has the potential inexpensively, and in a versatile way, to visualize and quantify the angiogeneic status of cardiovascular disease and tumors. The results of our present study indicate that PA imaging with the proposed low-cost $\alpha_v\beta_3$-targeted CuNPs can be applied to angiogenesis imaging in vivo. According to PA images acquired every 30 mins after the injection of CuNPs, an increasing number of angiogenic

sprouts and bridges between the mature vessels became visible as PA signals were enhanced within these vessels. This result was supported by an increasing value of the angiogenesis index, which is an indicator of the intensity of angiogenesis. The successful amplification of the PA signal after treatment requires binding of endothelial $\alpha_v\beta_3$-integrin receptors, which are sparsely distributed on the luminal aspect of quiescent endothelial cells[6], precluding the interactive binding of CuNPs to nonendothelial cells. The high specificity and binding affinity of this homing ligand is the key to the success.

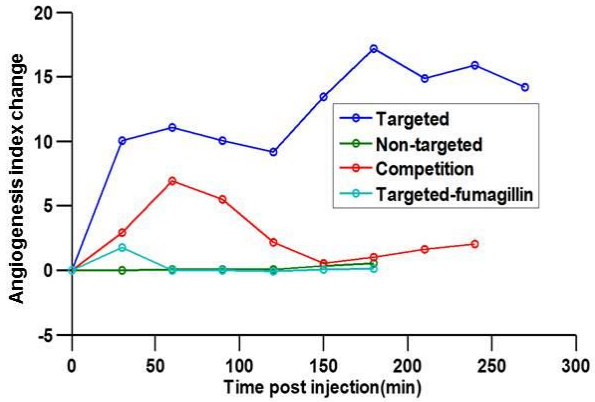


Fig. 5 Angiogenesis index versus time for four groups of mice.

PA imaging with contrast agents, such as dyes, gold nanoparticles, nanorods or nanocages has been reported previously. But these agents can diffuse out of neovessels easily and bind to numerous cell types (other than endothelial cells) with $\alpha_v\beta_3$-integrin. In contrast, the CuNPs in the present study can avoid such a "leaky" behavior and stay constrained within the Matrigel plug area, which is essential for quantitative purposes in a clinical study. The present study, to the best of our knowledge, is the first demonstration of PA imaging with CuNPs. With the inexpensive manufacturing, compared to the unpredictable and high cost of the existing gold nanoparticles, CuNPs have great potential for clinical use. However, it should also be noted that, there is still a long way to go before the clinical translation of CuNPs, considering the availability of clinical photoacoustic tomography scanners and the time required for investigational new drug approval.

## ACKNOWLEDGEMENTS

This research was supported by the National Institutes of Health Grants DP1 EB016986 (NIH Director's Pioneer Award), R01 EB008085, R01 CA134539, U54 CA136398, R01 CA159959. L.V.W. has a financial interest in Microphotoacoustics, Inc. and Endra, Inc., which, however, did not support this work.

## REFERENCES

[1] Wang, X., Xie, X., Ku, G. and Wang, L. V., "Noninvasive imaging of hemoglobin concentration and oxygenation in the rat brain using high-resolution photoacoustic tomography", J. Biomed. Opt., 11, 024015 (2006).

[2] Pan, D., Pramanik, M., Senpan, A., Allen, J. S., Zhang, H., Wickline, S. A., Wang, L. V. and Lanza, G. M., "Molecular photoacoustic imaging of angiogenesis with integrin-targeted gold nanobeacons", FASEB J., 25(3), 875-82 (2011).

[3] Lungu, G.F., Li, M.L., Xie, X, Wang, L.V. and Stoica, G., "In vivo imaging and characterization of hypoxia-induced neovascularization and tumor invasion", Int. J. Oncol., 30, 45-54 (2007).

[4] Ku, G., Wang, X. D., Stoica, G. and Wang, L. V., "Multiple-bandwidth photoacoustic tomography", Phys. Med. Biol., 49, 1329-1338 (2004).

[5] Schneider, B. P. and Miller, K.D., "Angiogenesis of breast cancer", J. Clin. Oncol., 23, 1782-1790 (2005).

[6] De-La-Zerda, A., Zavaleta, C., Keren, S., Vaithilingam, S., Bodapati, S., Liu, Z, Levi, J., Smith, B.R, Ma, T.J., Oralkan, O., Cheng, Z., Chen, X., Dai, H., Khuriyakub, B. T. and Gambhir, S. S., "Carbon nanotubes as photoacoustic molecular imaging agents in living mice", Nat. Nanotechnol., 3(9), 557-562 (2008).
[7] Wang, L. V. and Hu, S, "Photoacoustic tomography: in vivo imaging from organelles to organs", Science, Vol.335, No. 6075, 1458-1462 (2012).
[8] Pan, D, Pramanik, M., Senpan, A., Allen, J.S., Zhang, H., Wickline, S.A., Wang, L.V. and Lanza, G. M., ".Molecular photoacoustic imaging of angiogenesis with integrin-targeted gold nanobeacons", FASEB,Vol. 25, 876-882 (2011).
[9] Song, K.H. and Wang, L.V., "Deep reflection-mode photoacoustic imaging of biological tissue", J. Biomed. Opt., 12, 060503 (2007).
[10] Schmieder, A.H., Caruthers, S.D., Zhang, H., Williams, T.A., Robertson, J.D., Wickline, S.A. and Lanza, G.M., "Three-dimensional MR mapping of angiogenesis with alpha5beta1 (alpha nu beta3) targeted theranostic nanoparticles in the MDA-MB-435 xenograft mouse model", FASEB J., 22 (12): 4179-4189 (2008).